# Design of High Efficiency Circular Horns

Chan Kwok Kee
*Chan Technologies Inc.*
*15 Links Lane, Brampton, Ontario L6Y 5H1, Canada*
*Email: kwok-kee.chan@rogers.com*

**Abstract**

*Some aspects on the design of a high efficiency profiled circular horn are presented. The modal content at the circular aperture necessary to closely approximate a uni-polarized uniform distribution is first established. Slope discontinuities along the length of the horn are then used to generate the necessary aperture modes with the appropriate amplitudes and phases. The performance of the horn is calculated using the mode matching technique. Significant improvement in the aperture efficiency and reduction in the cross-polar level over a straight conical horn can be achieved. This conclusion is supported by the good agreement between predictions and measurements of a high efficiency dual-band horn.*

## 1. INTRODUCTION

For satellite communications, there is a requirement to provide multibeam coverage at both uplink and downlink frequency bands. The antenna of choice is a shaped reflector fed by multiple horns, with each horn forming a single beam. The main objectives in the antenna design are to increase the edge-of-coverage gain and reduce the co-polar and cross-polar interference from adjacent beams. The size of the reflector feed horn is restricted by the beam separation. Hence a good way of improving performance is to increase both the horn aperture and cross-polar efficiencies. Reducing the illuminating horn beamwidth substantially lowers the spillover loss and increases the edge taper of the reflector. Consequently, the edge-of-coverage gain of the secondary beam is raised. Further, the co-polar and cross-polar sidelobes are lowered thus increasing the inter-beam isolation. Improving these horn efficiencies can be achieved by introducing the appropriate kind and level of higher order modes at the horn aperture by means of circularly symmetric discontinuities along the horn. These discontinuities take the form of slope changes so that a smooth profiled horn results as shown in Fig. 1. The success of this approach has been verified by the close agreement between predictions and measurements of a high efficiency dual-band horn.

The steps necessary for the successive design of a multimode circular horn are as follows.

1. Determine the ideal modal content at the horn aperture, given the desired distribution.
2. Synthesize a profiled horn to give the desired radiation characteristics by means of optimization of horn physical parameters. Performance prediction is carried out using the mode matching technique.

These steps are discussed below.

## 2. DETERMINATION OF APERTURE MODAL CONTENT

The coefficients $A_i$ of the circular waveguide modes approximating a given aperture distribution *f(r)* are given by

$$A_i \propto \int_0^{2\pi}\int_0^{b} f(r)\,\hat{x}\bullet\overline{e}_i\; r\,dr\,d\phi \qquad (1)$$

where $\overline{e}_i$ is the electric field vector of the propagating circular waveguide modes and $\hat{x}$ is the polarization vector of the aperture distribution. The aperture distribution is assumed to be circularly symmetric and is perfectly polarized in the *x*-direction. The integration is taken over the horn aperture with radius *b*. Some of the types of distribution one may specify are the following.

Uniform:

$$f(r) = 1.0 \qquad (2)$$

Parabolic on a pedestal:

$$f(r) = pd + (1 - pd)\,[\,1 - \left(\frac{r}{b}\right)^2\,]^2$$

$$pd = 10^{**}(et/20)$$

Gaussian:

$$f(r) = \exp[\,\alpha(r/b)^2\,] \quad , \quad \alpha = et/8.6859$$

The edge taper is represented by *et* in dB (-ve). It is assumed that the horn is fed by a single-moded guide with the $TE_{11}$ mode. All the discontinuities are circularly symmetric. Consequently only the $TE_{1n}$ and $TM_{1n}$ modes can be excited. A list of these modes, together with the roots of their characteristic equations and the horn diameters where they are above cutoff, is given in Table 1. The x-components of these modes are given below.

$TE_{1n}$ modes:

$$e_{ix}^{h} = \sqrt{\frac{2}{\pi}}\,\sqrt{\eta_i^h}\;\frac{\chi_i^h}{\left[\left(\chi_i^h\right)^2 - 1\right]^{1/2}\; b\, J_1(\chi_i^h)}\left\{\begin{array}{l}\dfrac{J_1(\chi_i^h r/b)}{\chi_i^h r/b}\cos^2\phi\; + \\ J_1'(\chi_i^h r/b)\sin^2\phi\end{array}\right\}$$

$TM_{1n}$ modes:

$$e_{ix}^{e} = \sqrt{\frac{2}{\pi}}\,\sqrt{\eta_i^e}\;\frac{1}{b\, J_0(\chi_i^e)}\left\{\begin{array}{l}\dfrac{J_1(\chi_i^e r/b)}{\chi_i^e r/b}\sin^2\phi\; + \\ J_1'(\chi_i^e r/b)\cos^2\phi\end{array}\right\} \qquad (3)$$

The maximum aperture efficiency and minimum cross-polar level that can be achieved by a circular aperture with no phase error and the corresponding modal content should first be established. This was done by substituting eqn. (2) and (3) into (1) for a uniform and a -12 dB tapered distribution. The gain patterns of the aperture were computed using Kirchoff's vector diffraction integral from the aperture modal content. The aperture efficiency, peak cross-polar level and the number of propagating modes with non-zero excitations are plotted in Fig. 2, 3 and 4 respectively as a function of aperture diameter in wavelength. For the uni-polarized uniform distribution, only the $TE_{1n}$ modes are needed. For the tapered distribution both $TE_{1n}$ and $TM_{1n}$ modes are excited. The stair-case nature of these plots is caused by the presence of increasing number of higher order modes as these modes can only propagate at certain aperture diameter that is given in Table 1. Thus for a given aperture size, there is a maximum aperture efficiency that can be achieved. One can also achieve good cross-polar performance together with high aperture efficiency. The peak cross-polar level can be further reduced by sacrificing a bit of aperture efficiency.

## 3. SYNTHESIS OF PROFILED CIRCULAR HORNS

The method chosen here to excite the higher order modes employs slope discontinuity. This approach is found to have broader band performance than utilizing step discontinuity. The structure of a profiled horn with multiple discontinuities is shown in Fig. 1. The horn profile is linear in between the discontinuities. It is not possible to generate the TE modes without exciting the TM modes with a circular discontinuity. In practice, one can aim to control one or two higher order TE modes and minimize exciting the rest. Since only one or two higher order modes need to be generated and controlled in either one or two frequency bands, using 3 or 4 slope discontinuities should suffice. The discontinuity count excludes the one at the interface with the single moded input guide.

The design process involves specifying the approximate axial locations (al) of the slope break points and the radii (sr) of the horn cross-sections at these break points. The specified horn profile is then segmented into a series of stepped circular waveguide sections with varying radii. The horn is characterized by finding the generalized scattering matrices (GSM) of all the stepped waveguide junctions and then combining them together with those of the intervening waveguide sections to yield the overall scattering parameters. With the modal content at the aperture known, the radiation patterns can be readily calculated. The input return loss, peak cross-polar level and the efficiency of the horn at the specified frequencies (*i = 1, nfrq*) are used to form the objective function *F* given below, only if they are worse than the desired values.

$$F = \sum_{i=1}^{nfrq}\left\{wt_r\left(\rho_i - \rho_{di}\right)^2 + wt_x\left(xp_i - xp_{di}\right)^2 + wt_a\left(\eta_i - \eta_{di}\right)^2\right\} \qquad (4)$$

Here $\rho$, $xp$ and $\eta$ represent the return loss, peak cross-polar level in the diagonal plane, and aperture efficiency respectively. All these parameters are expressed in dB and the subscript $d$ indicates the desired value. The corresponding weights of the error functions are $wt_r$, $wt_x$ and $wt_a$. It should be noted that the weightings be set so that the error components are more or less of the same magnitude. An optimization routine minimizes the above objective function by searching for the optimum radii and locations of the slope breakpoints. This search is carried out within the limits of the optimization variables that are set by the user.

## 4. RESULTS

Simulations were carried out to determine how close one can come close to the theoretical limits shown in Fig. 2 by using a 3.71λ diameter horn at centre frequency. This horn has a 10.4% frequency bandwidth. Gain pattern cuts are plotted in Fig. 5 at the band edge and centre frequencies. The theoretical maximum efficiency is 94%. The best achievable efficiency is 91.6% which is quite close to the limit.

Figure 6 shows the breadboard horn that covers both the K and Ka bands and employs novel features to generate desired higher order modes. The horn has an aperture diameter of 2.27 in. and an axial length of 7.0 in. and uses finite number of discontinuities to generate higher order modes over the 18.3 /30.0 GHz bands. The measured versus computed radiation patterns of the horn are shown in Fig. 7. There is excellent correlation between the two. A minimum efficiency value of 84% to 85% is achieved across the K/Ka band frequencies. Measured return loss is better than 25 dB and peak cross-polar levels are between -20 to -26 dB relative to copolar peak. For comparison, same size Potter and corrugated horns have 70% and 52% efficiency values respectively. A significant increase in aperture efficiency has thus been achieved.

## REFERENCES

[1] S. Rao, K.K. Chan and M. Tang, "Dual-band multiple beam antenna system for satellite communications", IEEE Antenna & Propagation International Symposium, Washington, USA, Session 84, July 2005.

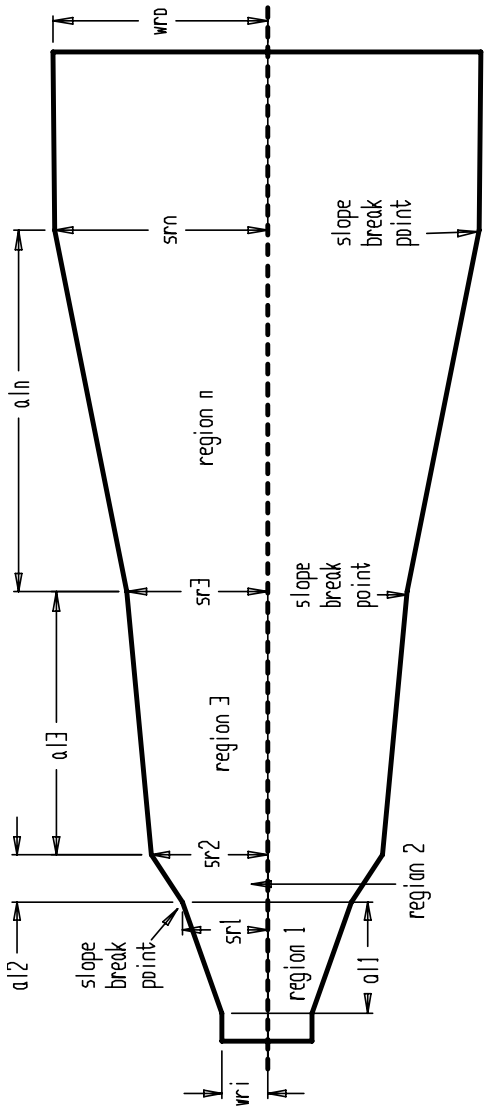


Fig. 1: Multi Mode Profiled Horn

Table 1: Circular Waveguide $TE_{1n}$ and $TE_{1n}$ Modes

| Mode | $\chi_{1n}$ root | Guide diameter ($\lambda$) |
|---|---|---|
| $TE_{11}$ | 1.841183 | 0.5861 |
| $TM_{11}$ | 3.831706 | 1.2197 |
| $TE_{12}$ | 5.331443 | 1.6971 |
| $TM_{12}$ | 7.015587 | 2.2331 |
| $TE_{13}$ | 8.536316 | 2.7172 |
| $TM_{13}$ | 10.17346 | 3.2383 |
| $TE_{14}$ | 11.70601 | 3.7261 |
| $TM_{14}$ | 13.32369 | 4.2411 |
| $TE_{15}$ | 14.86359 | 4.7312 |
| $TM_{15}$ | 16.47062 | 5.2428 |
| $TE_{16}$ | 18.01553 | 5.7345 |

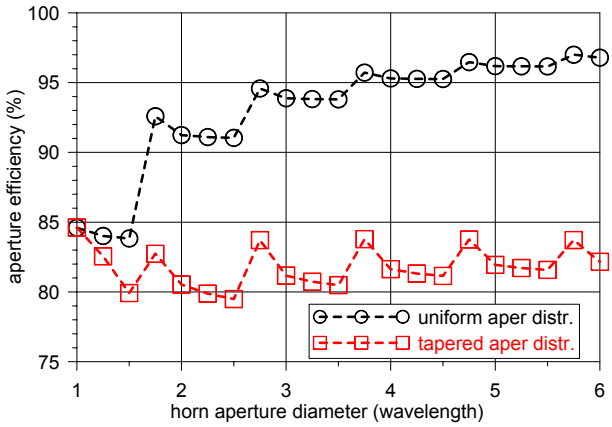


Fig. 2: Aperture efficiency of circular horn

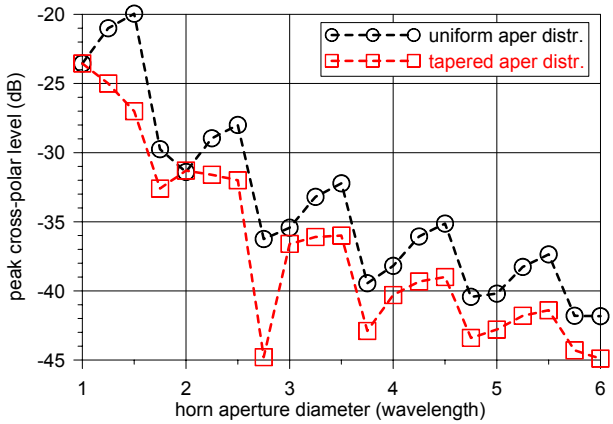


Fig. 3: Peak cross-polar level of circular horn

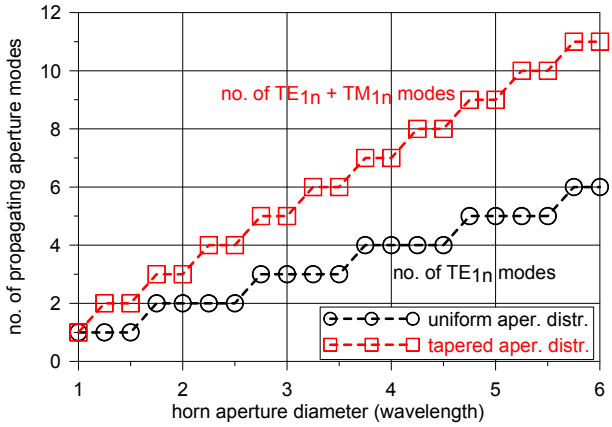


Fig. 4: Number of propagating $TE_{1n}$ & $TM_{1n}$ modes at circular aperture.

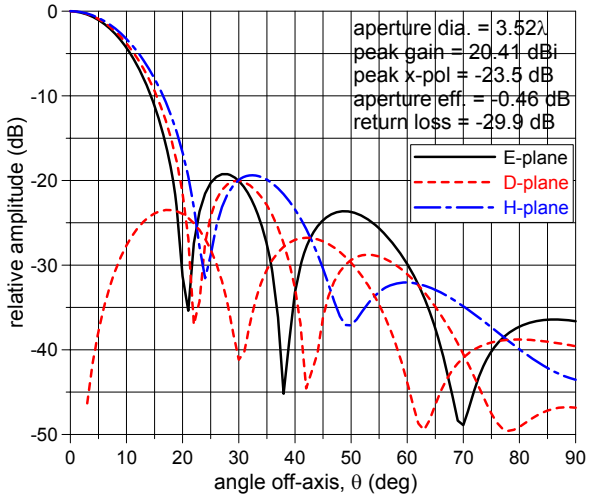


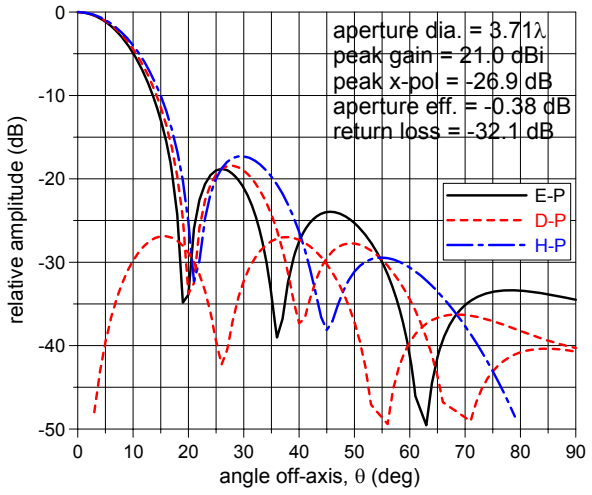


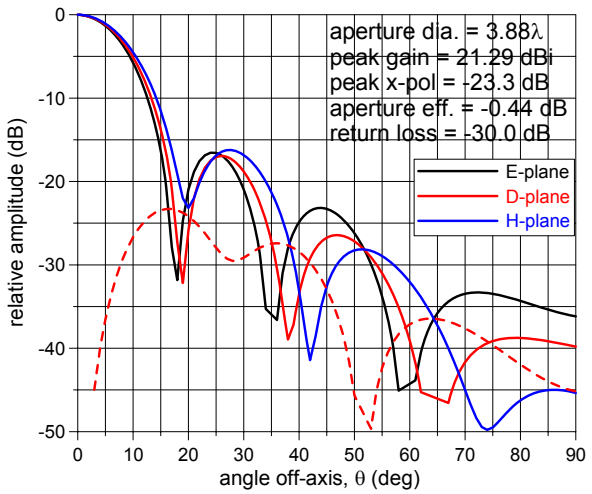


Figure 5: Pattern Cuts of a High Efficiency Horn with 10.4% bandwidth

Fig. 6: Breadboard Dual Band Horn

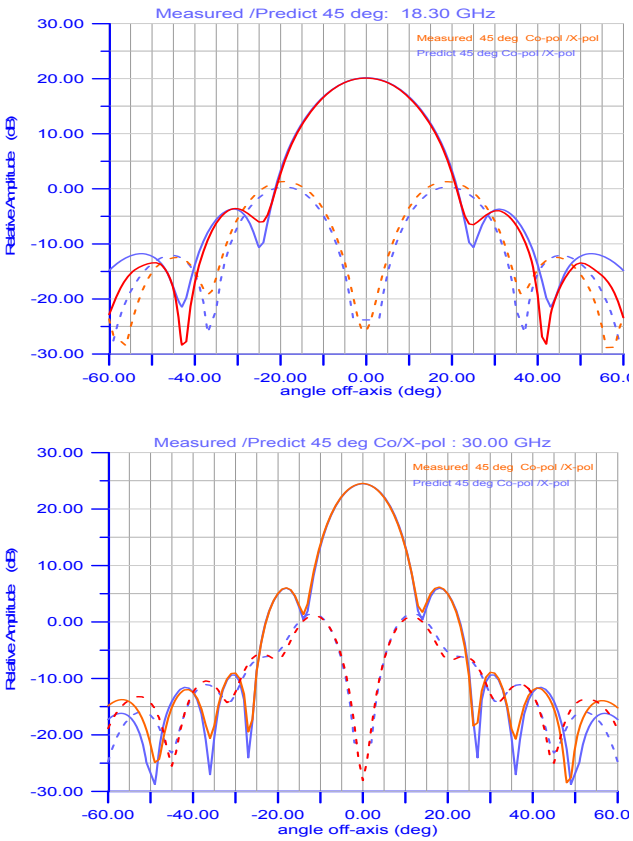


Fig. 7: Comparison between computed and measured gain patterns of a dual-band horn